# The Effects of the Atmospheric Medium on Wireless link Operating in the Millimeter Wavelengths and Terahertz Frequencies

Theodor Fedor Yudachev(1), Yosef Golovachev(2), Ya'akov Greenberg(3), Aviel Glam(3), Gad A. Pinhasi(4), and Yosef Pinhasi(1)
(1) Faculty of Engineering, Dept. of Electrical and Electronic Engineering, Ariel University, Ariel, 40700 Israel;e-mail: fiodor.yudachov@msmail.ariel.ac.il; yosip@ariel.ac.il
(2) Dept. of Electrical and Electronic Engineering, Jerusalem College of Technology, P.O. Box 16031, Jerusalem 91160, ISRAEL; e-mail: yosi_habad@yahoo.com
(3) RAFAEL Advanced Defense Systems; e-mail: YAACOVGR@rafael.co.il; AVIELG@rafael.co.il
(4) Dept. of Chemical Engineering, Ariel University, Ariel, 40700 Israel; e-mail: gadip@ariel.ac.il

## Abstract

This study presents an analytical framework for evaluating the cumulative effects of attenuation, phase dispersion, and group delay in millimeter and sub-millimeter wave propagation from Earth to space, particularly in the Extremely High Frequencies (EHF) (30 GHz–300 GHz) band. These frequencies enable ultra-wideband communication and high-resolution remote sensing but are strongly influenced by meteorological phenomena. Analyses described in the study are based on cumulative levels calculated by the Millimeter-Wave Propagation Model (MPM) with a non-uniform atmospheric refractivity profile to account for altitude-dependent signal degradation. Atmospheric absorption, water vapor scattering, fog, clouds, precipitation, and air pressure variations strongly affect the cumulative attenuation, phase distortion, and timing delays, impacting link budget performance. The influence of meteorological factors is most pronounced in the lower atmospheric layers, where humidity and precipitation induce significant variations. However, these effects may persist at higher altitudes under anomalous conditions. This refined methodology advances our understanding of high-frequency communication constraints and provides a robust foundation for optimizing wireless links, enhancing their resilience across diverse environmental conditions.

## 1 Introduction

The increasing demand for high-data-rate communication has accelerated the adoption of satellite systems' millimeter and sub-millimeter wave frequencies. The EHF band offers access to underutilized wideband channels, making it highly suitable for satellite communication, remote sensing, and next-generation radar applications [1]. However, electromagnetic wave propagation at these frequencies is strongly influenced by atmospheric interactions, including selective absorption, scattering, and phase distortion. Unlike lower frequency bands, where free-space propagation dominates, EHF signals experience significant frequency-dependent attenuation due to molecular absorption, particularly by oxygen and water vapor. Additional degradation occurs in the presence of clouds, fog, and precipitation, leading to further signal losses and scattering effects [5]. Research highlights significant absorption peaks at 22 GHz and 183 GHz (water vapor) and 60 GHz and 119 GHz (oxygen resonance), posing severe challenges to transmission efficiency (Figure 1)[5].

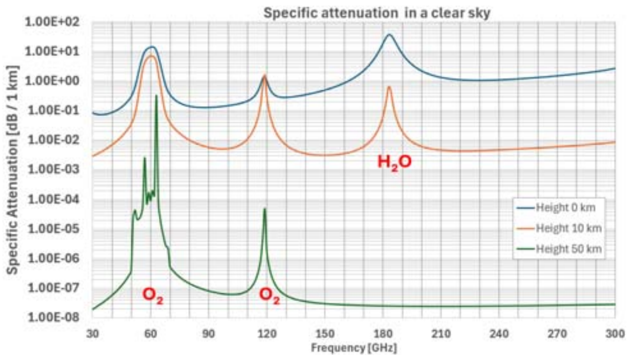


**Figure 1.** Attenuation analysis at altitudes of 0, 10 km and 50 km in a clear sky

Beyond attenuation, refraction created in the atmosphere also affects the propagation of the electromagnetic signal. The refractive index of air varies with altitude, humidity, and temperature [4]. In this work, we employ the millimeter wave propagation model (MPM) [2] for the evaluation of the atmospheric vulnerability $\chi(f)$ (atmospheric sensitivity) and the complex index of refraction of the air:

$$n(f) = \sqrt{1+\chi_e'(f) - j\chi_e''(f)} \approx 1 + \underbrace{\frac{1}{2}\chi_e'(f)}_{[N_0+N'(f)]\cdot 10^{-6}} - j\underbrace{\frac{1}{2}\chi_e''(f)}_{N''(f)\cdot 10^{-6}} \quad (1)$$

This enables the calculation of the local attenuation factor $\alpha(f)$, wavenumber $\beta(f)$, and the resulting group delay $\tau_g(f)$ [per km] [2]:

$$\alpha(f) = \frac{2\pi f}{c} N''(f) \times 10^{-6} \tag{2}$$

$$\beta(f) = \frac{2\pi f}{c} \left[1 + N'(f)\right] \times 10^{-6} \tag{3}$$

$$\tau_g(f) = \frac{1}{2\pi}\frac{d\beta(f)}{df} + \frac{1}{c}\left[N'(f) + f \cdot \frac{1}{f} N''(f)\right] \times 10^{-6} \tag{4}$$

The local parameters are used for the calculation of the cumulative attenuation and delay along the propagation path for different communication scenarios, including those where the wave is propagating in an inhomogeneous medium, for which the refractive index is not constant [3]. We demonstrate the impact of a non-uniform atmospheric refractivity on the propagation path and the link budget of Earth-to-space satellite links operating in the millimeter and terahertz wave regimes[6].

## 2 Cumulative Attenuation Analysis

As the electromagnetic signal progresses through the atmosphere, it encounters varying densities and compositions of gases. At lower altitudes, where air density is highest, interactions with oxygen and water vapor dominate, leading to substantial molecular absorption [7]. The incremental loss at the i'th segment is thus:

$$\cos(\theta_i) = \frac{R_E}{R_E + h} \cdot \frac{n_r(0)}{n_r(h)} \cdot \cos(\theta_0), \tag{5}$$

where $R_E$ is the Earth's radius, $h$ is the altitude, $\theta_0$ is the initial elevation angle, and $\theta_i$ is the refracted angle at altitude $h$ [2] . This bending causes lower elevation angles to have longer path lengths and increased atmospheric interactions, which leads to more significant cumulative attenuation[1] .

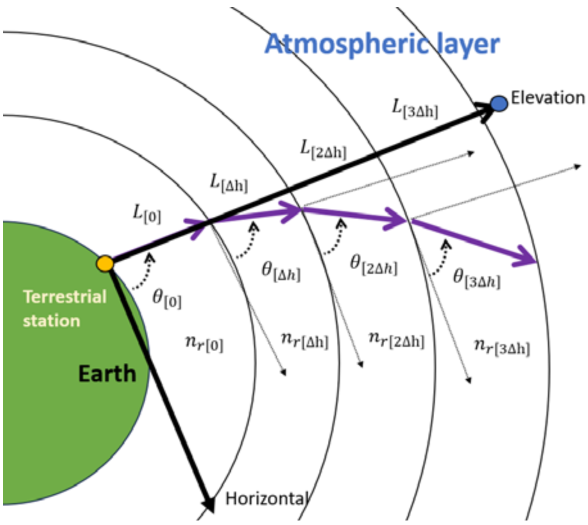


**Figure 2.** Optical path through the atmosphere layers

As the electromagnetic signal progresses through the atmosphere, it encounters varying densities and compositions of gases. At lower altitudes, where air density is highest, interactions with oxygen and water vapor dominate, leading to substantial molecular absorption [7] . The incremental loss at the i'th segment is thus:

$$\Delta L_i(h) = e^{2\alpha(h,f)\cdot\frac{\Delta h}{sin(\theta_i)}} \cong exp\left\{\frac{2\cdot\alpha(h,f)\cdot h}{\sqrt{1-\left[\frac{n_r(0)}{n_r(i\cdot\Delta h)}\right]cos(\theta_0)^2}}\right\} \tag{6}$$

The cumulative attenuation is a result of the summation:

$$L(h) \cong \sum_{\mathrm{i}} \Delta L_i(h) \tag{7}$$

where $\Delta L_i(h)$ represents the contribution of an atmospheric layer at altitude $h$, and $\alpha(f, R(h))$ is the local specific attenuation due to rain. This attenuation depends on both frequency $f$ and rain rate $R(h)$, and is modeled using the Millimeter-wave Propagation Model (MPM) [2]:

$$\gamma_{\mathrm{MPM}}(f,R) = \frac{R\cdot(3.7+0.012R)\cdot\left(\frac{f}{f_R}\right)^{2.5}}{f_R\cdot\left[1+\left(\frac{f}{f_R}\right)^{2.5}\right]} \tag{8}$$

with the rain resonance frequency defined as:

$$f_R = 53 - R\cdot(0.37 - 0.0015R) \tag{9}$$

This model captures the nonlinear dependence of attenuation on both frequency and rainfall intensity. Attenuation increases rapidly in the millimeter and sub-millimeter wave bands, particularly above 30 GHz, as illustrated in Figure 3.

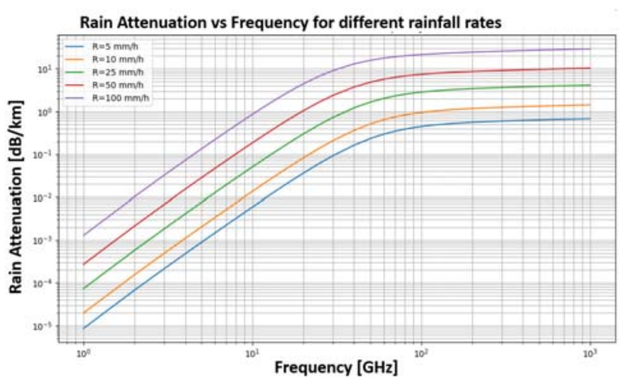


**Figure 3.** Rain attenuation vs. frequency for different rainfall rates. Higher frequencies exhibit exponential growth in attenuation as rainfall rate increases.

Both fog and cloud cover, like rain, influence the level of signal attenuation. Below are two graphs illustrating the total attenuation over a distance of 100 km above the ground under various meteorological conditions. Figure 4 displays the transmission mode that is perpendicular to the Earth's surface, while Figure 5 shows the transmission mode at a 60° angle to the Earth, which effectively increases the total distance the signal travels.

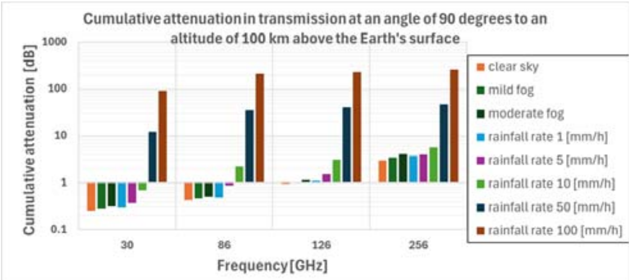


**Figure 4.** Cumulative attenuation in transmission at an angle of 90 degrees to an altitude of 100 km above the Earth's surface.

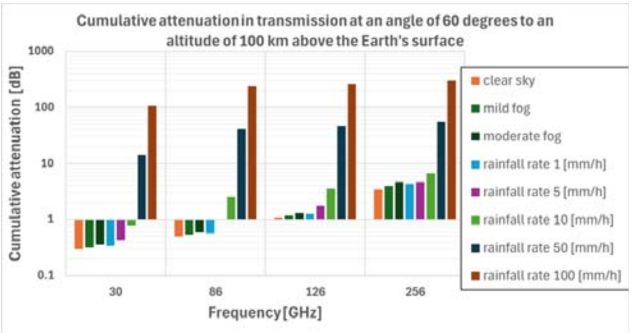


**Figure 5.** Cumulative attenuation in transmission at an angle of 60 degrees to an altitude of 100 km above the Earth's surface.

The propagation of signals at EHF) is significantly influenced by the geometry of the transmission and the meteorological conditions affecting the signal as it crosses from the transmission point to the reception point, particularly when directing signals toward a satellite. Understanding the attenuation values caused by atmospheric conditions is crucial, as it impacts the calculation of the link budget for the ground station in relation to the satellite. [1].

## 3 Cumulative Phase Dispersion Analysis

Atmospheric pressure, temperature variations, and water vapor content affect the refractive index, causing differential phase dispersions that degrade signal coherence, particularly in the 30–300 GHz range. Phase dispersion, measured in degrees per kilometer, depends on frequency and atmospheric conditions. The MPM approximates phase dispersion as:

$$\beta = 1.2008 f N'(f) \tag{10}$$

where $N'(f)$ is the real part of the complex refractivity, and $f$ is the frequency in GHz. This equation highlights the frequency-dependent nature of phase dispersion, with stronger effects at higher frequencies. Gaseous absorption by atmospheric oxygen and water vapor affects phase dispersion. The absorption coefficients vary with frequency, significantly impacting millimeter-wave propagation. The total phase dispersion incorporates these contributions and can be computed using:

$$N' = N'_{\text{dry}} + N'_{\text{vapor}} + N'_c \tag{11}$$

where $N'_{\text{dry}}$ represents the dry air refractivity, $N'_{\text{vapor}}$ accounts for water vapor effects, and $N'_c$ is an empirical correction for continuum absorption.

The following table 1 summarizes phase dispersion values for different environments:

**Table 1.** Phase Dispersion (PD) Table

| Location | Freq (GHz) | P.D. (deg/km) | P.D. (deg/MHz) |
|---|---|---|---|
| Desert | 30 | 169.49 | 1.69490 |
| Desert | 60 | 7.52 | 0.03760 |
| Desert | 100 | 195.98 | 0.58794 |
| Tropical | 30 | 319.88 | 3.19880 |
| Coastal | 50 | 58.34 | 0.35004 |

The following figure illustrates the cumulative phase dispersion across different transmission angles, measured at an altitude of 100 km above Earth's surface. The graph emphasizes the significant variability in phase dispersion as a function of frequency and transmission angle.

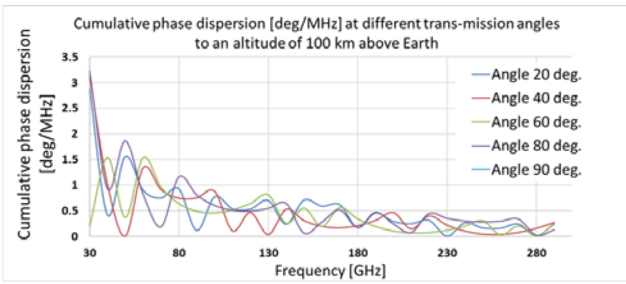


**Figure 6.** Cumulative phase dispersion at different transmission angles to an altitude of 100 km above Earth's surface in clear sky.

Based on the results in Graph 6, as the frequency increases, the total phase dispersion decreases up to a distance of 100 km towards space. The transmission angle has limited influence under the tested conditions. From the results in Table 1, it is clear that meteorological conditions, particularly the levels of water vapor in the air (W.V.), influence the angular deviation. The calculations were performed assuming a water vapor level of approximately 5 g/m$^3$ in the desert and around 25 g/m$^3$ in a tropical region.

## 4 Cumulative Group Delay

Cumulative group delay ($\tau_{cum}$) refers to the total accumulated delay experienced by a signal as it propagates from Earth to space. This delay is influenced by various atmospheric factors such as temperature, humidity, and pressure, which affect the refractive index of the atmosphere. The total group delay is obtained by integrating the local group delay $\tau_g(h)$ over the entire transmission path:

$$\tau_{cum} = \int_0^L \tau_g(h)dh \qquad (12)$$

where $h$ represents the altitude-dependent atmospheric properties, $L$ is the total propagation path length and $\tau_g(h)$ is the local group delay at altitude $h$. The group delay at a given altitude is determined by:

$$\tau_g = 3.336N(f) \quad \text{[ps/km]} \qquad (13)$$

where $N(f)$ is the frequency-dependent refractivity, incorporating contributions from dry air, water vapor, and pressure effects [5] and coefficient 3.336 arises from the relation between refractivity and speed of light. In satellite communications, the cumulative group delay varies based on the elevation angle of transmission. Below is an example of a cumulative group delay analysis for a signal propagating to an altitude of 100 km at different transmission angles. A smaller transmission angle results in a longer signal path through the atmosphere as shown in Figure 7.

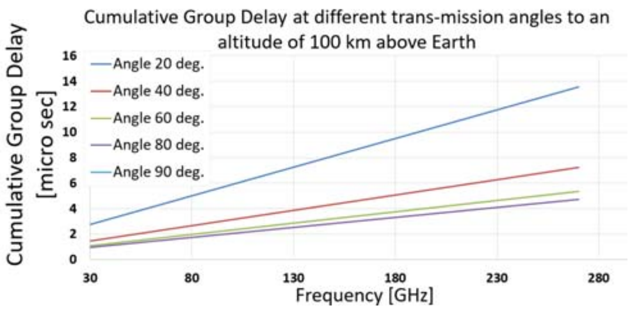


**Figure 7.** Cumulative group delay for different elevation angles in a clear sky condition

Understanding cumulative group delay is crucial for maintaining synchronization in satellite-based systems such as GPS, deep-space communication, and Inter-Satellite Links (ISL).

## 5 Conclusion

This paper aims to provide a general overview of the combined impact of atmosphere on propagation of higher frequency signals, namely, through the presentation of synergy effects covering attenuation, phase dispersion and group delay of EHF signals. As shown, atmospheric gases, humidity, and precipitation have a strong effect at low altitudes drastically reducing signal intensity and coherence. By means of analytical modeling based on the Millimeter-wave Propagation Model (MPM), we also assessed how the frequency, the elevation angle and the meteorological profile affect the propagation path. We demonstrated that attenuation rises very quickly with frequency, that phase delay dispersion is highly water vapor dependent, and that group delay is markedly elevation angle dependent. These results are essential for engineers planning and designing satellite communication systems operating above 30 GHz, including applications in next-generation high-throughput satellites (HTS), ISL, Earth observation sensors, and beyond-5G/6G backhaul. The developed framework enables engineers to perform more accurate link budget analysis and predict dynamic atmospheric effects such as rain fade and cloud-induced signal dispersion. Future work will focus on testing prototypes under severe storm conditions and add measurements of polarization shifts .

## References

[1] E. Cianca, T. Rossi, A. Yahalom, Y. Pinhasi, J. Farserotu, and C. Sacchi, "EHF for Satellite Communications: The New Broadband Frontier," *Proceedings of the IEEE*, **99**, 11, November 2011, pp. 1858–1876, doi:10.1109/JPROC.2011.2158765.

[2] H. J. Liebe, "MPM—An Atmospheric Millimeter-Wave Propagation Model," *International Journal of Infrared and Millimeter Waves*, **10**, 6, June 1989, pp. 631–650, doi:10.1007/BF01009565.

[3] Y. Golovachev, A. Etinger, G. A. Pinhasi, and Y. Pinhasi, "Propagation Properties of Sub-millimeter Waves in Foggy Conditions for Satellite Applications," *Journal of Applied Physics*, **125**, 15, April 2019, doi:10.1063/1.5083711.

[4] D. Misra, D. K. Misra, and S. P. Tripathi, "Satellite Communication Advancement, Issues, Challenges, and Applications," *International Journal of Advanced Research in Computer and Communication Engineering*, **2**, 4, April 2013, pp. 1681–1686.

[5] Y. Balal and Y. Pinhasi, "Atmospheric Effects on Millimeter and Sub-millimeter (THz) Satellite Communication Paths," *Journal of Infrared, Millimeter, and Terahertz Waves*, 2018, doi:10.1007/s10762-018-0554-7.

[6] Y. Golovachev, G. A. Pinhasi, and Y. Pinhasi, "Atmospheric Effects on OFDM Wireless Links Operating in the Millimeter Wave Regime," *Electronics*, **9**, 10, September 2020, pp. 1598, doi:10.3390/electronics9101598.

[7] L. J. Ippolito, "Attenuation of Electromagnetic Radiation by Haze, Fog, Clouds, and Rain," *Proceedings of the IEEE*, **72**, 11, November 1984, pp. 1368–1379, doi:10.1109/PROC.1984.13086.